Revista Mexicana de Astronomía y Astrofísica, **47**, 333–344 (2011)

THE PROPER MOTION OF THE LARGE MAGELLANIC CLOUD REVISITED

M. H. Pedreros[1,2]

Received 2011 March 2; accepted 2011 June 24

RESUMEN

El movimiento propio (PM) de la Nube Mayor de Magallanes (LMC) relativo a cuatro cuasares en el trasfondo de los respectivos campos, se ha determinado leyendo y reprocesando datos de las imágenes de dos estudios previos. El PM total del centro de masas de la LMC que se obtiene aquí es $\mu = (+1.94 \pm 0.08)$ mas yr^{-1}, con un ángulo de posición de $\theta = (61.5 \pm 3.2)^\circ$. Los nuevos resultados concuerdan razonablemente con aquellos obtenidos previamente por nuestro y otros grupos, y con varios modelos teóricos existentes. A partir de la velocidad radial del centro de la LMC obtenida de la literatura, en combinación con el vector velocidad transversal determinado de nuestra medición del PM en este trabajo, obtenemos la velocidad espacial del centro de la LMC. Usando esta última y suponiendo un potencial puntual de masa para la Galaxia, hemos estimado la cantidad de masa contenida dentro de 50 kpc desde el centro de la Galaxia.

ABSTRACT

The proper motion (PM) of the Large Magellanic Cloud (LMC) relative to four background quasi-stellar objects has been determined by reading and reprocessing image data from two previous studies. The total center of mass PM for the LMC obtained here is $\mu = (+1.94 \pm 0.08)$ mas yr^{-1}, with a position angle $\theta = (61.5 \pm 3.2)^\circ$. The new results agree reasonably well with those obtained previously by our group and by other groups, and with several existing theoretical models. From the radial velocity of the center of the LMC found in the literature, in combination with the transverse velocity vector determined from the PM measured in the present work, we obtain the space velocity of the LMC center. Using the latter and assuming a point-mass potential for the Galaxy, we have estimated the amount of mass contained within 50 kpc of the center of the Galaxy.

Key Words: astrometry — proper motions — Magellanic Clouds — quasars: general

1. INTRODUCTION

The present study is a follow-up of the works by Anguita, Loyola, & Pedreros (2000, hereafter ALP00), Pedreros, Anguita, & Maza (2002, hereafter PAM02), Pedreros, Costa, & Méndez (2006, hereafter PCM06) and Costa et al. (2009, hereafter CMP09), in which the PM of the LMC was determined using the "quasar method". This method, fully described in ALP00, PAM02 and PCM06, consists in using quasi-stellar objects (QSOs) in the background field of the LMC as fiducial reference points to determine the PM of the cloud. In this method, the position of the background QSOs is measured at different epochs with respect to a group of bona-fide field stars of the LMC (the Local Reference System, hereafter LRS). Because a QSO can be considered a fiducial

[1]Departamento de Física, Facultad de Ciencias, Universidad de Tarapacá, Arica, Chile.

[2]Visiting Astronomer, Cerro Tololo Inter-American Observatory, National Optical Astronomy Observatories, operated by the Association of Universities for Research in Astronomy, Inc. (AURA), under cooperative agreement with the National Science Foundation.

TABLE 1

PREVIOUS DETERMINATIONS OF THE LMC PROPER MOTION BY OUR GROUP USING THE QUASAR METHOD

Source	$\mu_\alpha \cos(\delta)$ mas yr^{-1}	μ_δ mas yr^{-1}	Weighted Mean from
ALP00 (LMC center)	$+1.7 \pm 0.2$	$+2.9 \pm 0.2$	Three fields
PAM02 (LMC center)	$+2.0 \pm 0.2$	$+0.4 \pm 0.2$	One Field
PCM06 (LMC center)	$+1.8 \pm 0.1$	$+0.9 \pm 0.1$	Four fields
CMP09 (LMC center)	$+1.82 \pm 0.13$	$+0.39 \pm 0.15$	One field

TABLE 2

OBSERVATIONAL MATERIAL FOR THE LMC QSO FIELDS

Field	Source	Epochs	Frames	Epoch Range
Q0459-6427	PAM02	9	45	1989.91−2001.96
Q0557-6713	ALP00	13	70	1989.02−2001.96
Q0558-6707	ALP00	9	48	1992.81−2001.96
Q0615-6615	ALP00	11	53	1989.90−2001.96

reference point, any motion detected will be a reflexion of the motion of the LRS, that is, those selected LMC stars present in each field.

As shown in Table 1, and despite the fact that basically the same set of images was used in the mentioned studies (excepting the case of CMP09, as explained in item 6 of § 6), there is a rather large discrepancy, particularly in DEC, between the PM of the LMC derived by ALP00 and that derived by PAM02 and PCM06, with ALP00-PCM06 differences of -0.1 mas yr^{-1} (0.7σ) in R.A., and $+2.0$ mas yr^{-1} (13σ) in DEC This puzzle prompted us to read and re-process directly the original images obtained by ALP00 and PAM02 along with those added in PCM06 and not taken into account in the two previously mentioned works. This is because, as mentioned in PCM06, all previous analyses were carried out using not the original image material but rather the (X, Y) coordinates processed by the original authors, with the exception of the newly processed data not included in ALP00 and those included in PAM02. Therefore the results reported here were determined using the (X, Y) coordinates directly obtained from the re-processing of the LMC images themselves of the QSO fields containing: Q0459-6427, Q0557-6713, Q0558-6707 and Q0615-6615 (in the same nomenclature used by PCM06). The original study of field Q0459-6427 was reported in PAM02, and those of Q0557-6713, Q0558-6707 and Q0615-6615 in ALP00 and PCM06. Table 2 summarizes the total observational material used in the present work. The new processing led to a different number of frames, from those for the same fields in PCM06, because of the deletion of one or two frames due to a bad quality image or other reasons, which became apparent with the new inspection of the images required for their new processing. In one case (Q0615 field) three frames were added to the previous sample, which were not considered before. We will refer to CMP09 in § 6, because it is a special case, with a different set of images.

2. OBSERVATIONS AND REDUCTIONS

The observational material used in this work was described in ALP00, PAM02 and PCM06 and was obtained at the Cassegrain focus of the CTIO 1.5 m telescope in its f/13.5 configuration. The CCD chips used in each epoch for each field are shown in Table 3. The same LRS stars and numbering were adopted as those used by ALP00 or PAM02. The number of LRS stars in each of the studied fields is 17, 23, 52 and 16, for the fields Q0459-6427, Q0557-6713, Q0558-6707 and Q0615-6615, respectively. Finding charts for the reference stars and the background QSO in each field can be found in ALP00 and PAM02.

TABLE 3

MEAN BARYCENTRIC POSITIONS OF QUASARS IN THE LMC

Epoch	$\Delta\alpha\cos(\delta)$ arcsec	σ mas	$\Delta\delta$ arcsec	σ mas	N	CCD chip
			Q0459-6427			
1989.908	8.433	1.0	−7.612	2.6	3	RCA No.5
1990.872	8.434	2.2	−7.620	5.9	3	Tek No. 4
1990.878	8.427		−7.620		1	RCA No.5
1993.800	8.429	0.9	−7.613	4.0	3	Tek1024 No.1
1993.953	8.437	1.1	−7.610	1.9	9	Tek1024 No.2
1994.916	8.427	1.3	−7.614	2.4	3	Tek1024 No.2
1996.860	8.429	3.8	−7.618	1.5	5	Tek2048 No.4
1998.880	8.424	1.4	−7.615	1.2	6	Tek1024 No.2
2000.010	8.421	0.7	−7.616	1.1	9	Tek1024 No.2
2001.961	8.422	1.5	−7.611	2.4	3	Tek1024 No.2
			Q0557-6713			
1989.024	0.048	0.9	−2.770	0.9	6	RCA No.5
1989.905	0.037	1.3	−2.772	1.8	8	RCA No.5
1990.873	−0.036	0.8	−2.772	0.8	5	Tek No. 4
1990.878	−0.045	3.7	−2.769	0.6	2	RCA No.5
1991.938	0.043	1.7	−2.772	1.0	6	Tek1024 No.1
1992.812	0.037	0.6	−2.776	1.5	5	Tek 2048 No.1
1993.055	0.034	2.1	−2.776	1.2	3	Tek1024 No.1
1993.800	0.042	0.0	−2.779	0.0	1	Tek1024 No.1
1993.953	0.036	0.8	−2.779	1.1	9	Tek1024 No.2
1994.119	0.032	1.0	−2.779	1.3	5	Tek1024 No.2
1994.917	0.034	0.8	−2.784	0.8	9	Tek1024 No.2
1996.861	0.031	0.7	−2.781	0.9	3	Tek 2048 No.4
1998.883	0.032	0.4	−2.789	0.8	6	Tek1024 No.2
2001.961	0.029	0.3	−2.786	0.8	3	Tek1024 No.2
			Q0558-6707			
1991.939	−12.230	1.3	−15.479	0.2	3	Tek1024 No.1
1992.813	−12.232	4.7	−15.475	4.3	4	Tek2048 No.1
1993.058	−12.229	0.5	−15.482	1.0	4	Tek2048 No.1
1993.952	−12.231	0.7	−15.480	1.8	6	Tek1024 No.2
1994.117	−12.240	1.4	−15.486	0.7	3	Tek1024 No.2
1994.918	−12.234	0.5	−15.485	1.1	7	Tek1024 No.2
1996.863	−12.235	1.8	−15.486	1.8	6	Tek2048 No.4
1998.886	−12.239	0.6	−15.489	0.8	3	Tek1024 No.2
1999.942	−12.240	0.9	−15.489	1.0	6	Tek1024 No.2
2001.958	−12.243	1.3	−15.485	1.2	6	Tek1024 No.2
			Q0615-6615			
1989.908	−7.294	3.3	−8.078	2.1	3	RCA No.5
1990.878	−7.297	3.7	−8.082	1.2	3	RCA No.5
1993.954	−7.286	2.5	−8.089	2.0	7	Tek1024 No.2
1994.920	−7.279	2.3	−8.090	1.1	4	Tek1024 No.2
1995.178	−7.277	1.0	−8.092	1.0	3	Tek1024 No.2
1996.069	−7.282	3.1	−8.090	3.3	3	Tek1024 No.2
1996.864	−7.280	2.6	−8.085	0.9	3	Tek2048 No.4
1997.194	−7.280	2.0	−8.090	2.9	5	Tek1024 No.2
1998.886	−7.273	2.8	−8.098	2.0	3	Tek1024 No.2
1999.942	−7.271	1.0	−8.093	1.4	3	Tek1024 No.2
2001.959	−7.269	1.3	−8.100	1.3	15	Tek1024 No.2

The method we used for the LMC PM determination was previously explained in PCM06. In brief, after obtaining the (x, y) coordinates of the QSO and the LMC field reference stars in each image (the LRS), using a sequence of DAOPHOT's routines (Stetson 1987), the coordinates were corrected for differential color refraction (DCR) and transformed to barycentric coordinates, that is, $(x - \overline{x}, y - \overline{y})$ coordinates relative to the average

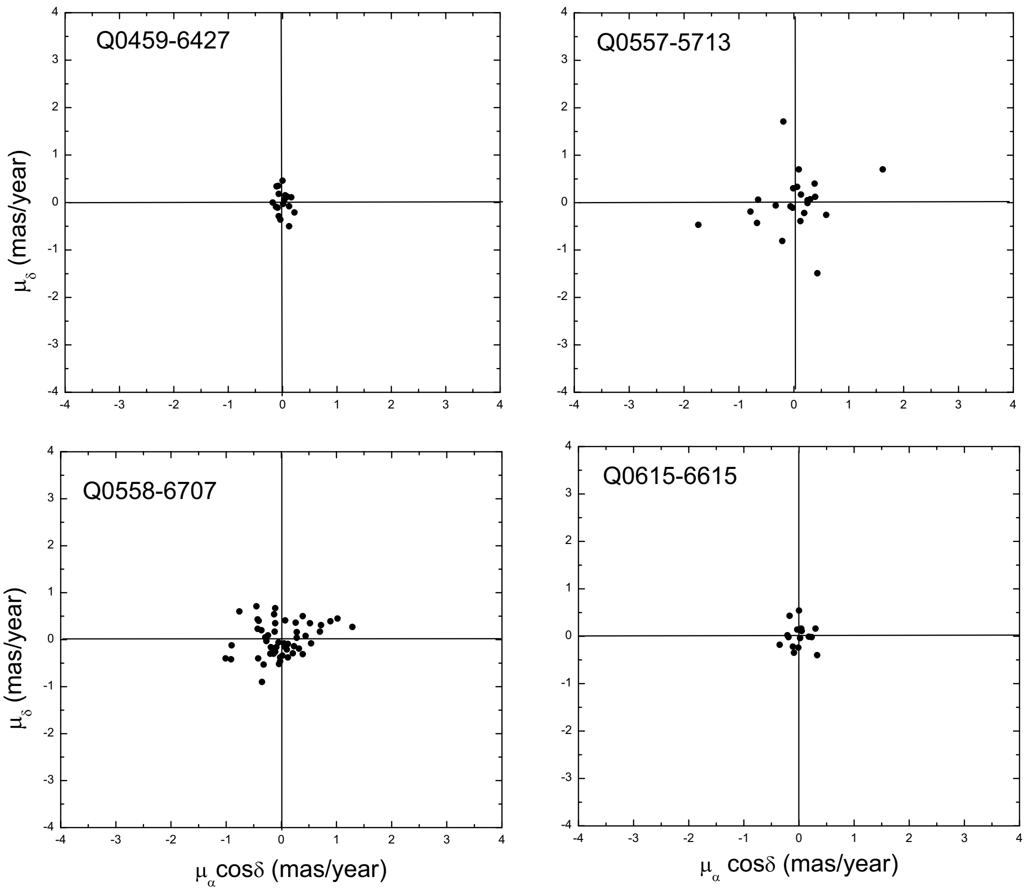

Fig. 1. Residual proper-motion maps for the reference stars. The dispersion around the mean is ±0.11, ±0.62, ±0.46, and ±0.19 mas yr^{-1} in R.A. ($\mu_\alpha \cos\delta$), and ±0.26, ±0.60, ±0.36, ±0.26 mas yr^{-1} in DEC (μ_δ), for Q0459-6427, Q0557-6713, Q0558-6707 and Q0615-6615, respectively.

($\overline{x}, \overline{y}$) coordinates of the LRS stars in the image. Then, by averaging the barycentric coordinates of the best set of consecutive images taken for each QSO field throughout our program, a Standard Reference Frame (SRF) was defined for every field. Later on, all images of each field, taken at different epochs, were referred to its corresponding SRF (one per field). This registration process was done through a multiple regression analysis by fitting both sets of coordinates to a third degree polynomial of the form:

$$X = a_0 + a_1x + a_2y + a_3x^2 + a_4xy + a_5y^2 + a_6x^3 + a_7x^2y + a_8xy^2 + a_9y^3\,,$$

$$Y = b_0 + b_1x + b_2y + b_3x^2 + b_4xy + b_5y^2 + b_6x^3 + b_7x^2y + b_8xy^2 + b_9y^3\,,$$

where (X, Y) are the coordinates on the SRF system and (x, y) are the the observed barycentric coordinates. It was found that the above transformation equations yielded the best results for the registration into the SRF, showing no remaining systematic trends in the data. It must be noted here that in the previous studies of the fields mentioned above, quadratic and linear polynomials were adopted instead, for the registration into the SRF.

3. RESULTS

The results for the LRS stars are much improved (with the significant lower dispersion shown below), in comparison to those obtained by PCM06 and shown in their Tables 3–6. In Figure 1 we present the PM (μ) maps for the LRS stars obtained in this work. The dispersion around the mean in the figure turned out to be (in parentheses the values by PCM06) ±0.11 (±0.34), ±0.62 (±0.79), ±0.46 (±0.54), and ±0.19 (±0.41) mas yr^{-1}

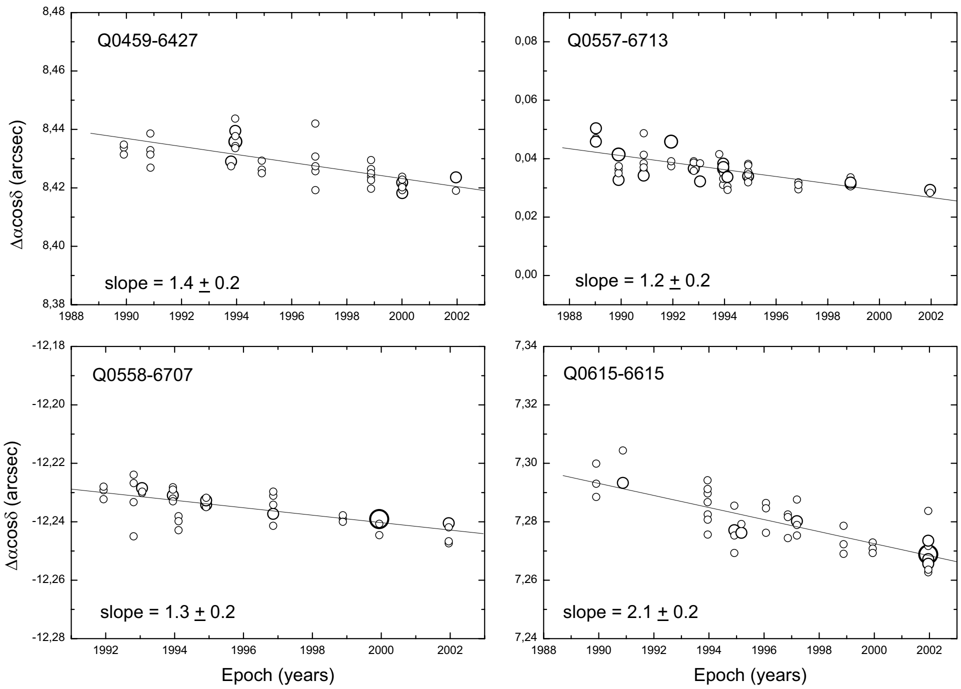

Fig. 2. Relative positions in R.A. ($\Delta\alpha\cos\delta$) vs. epoch of observation for the studied fields. The values of $\Delta\alpha\cos\delta$ represent the individual positions of the QSO on different CCD frames relative to the barycenter of the SRF. The point sizes are proportional to the number of times the measurement yielded the same coordinate value for a particular epoch (extra-small, small, medium, large and extra-large sizes indicate one to five measurements per epoch, respectively). The best-fit straight lines from linear regression analyses on the data are also shown.

in R.A., and ±0.26 (±0.52), ±0.60 (±0.71), ±0.36 (±0.58), ±0.26 (±0.62) mas yr^{-1} in DEC, for Q0459-6427, Q0557-6713, Q0558-6707 and Q0615-6615, respectively.

We believe the improvement is mainly due to the new third degree polynomial registration process used in the present work. It seems that the latter is quite adequate for the optics of the telescope we used, which, by the way, was never changed throughout the entire time baseline of this project. As stated in PCM06, we believe the scatter shown in the plots probably stems entirely from the random errors in the measurements and the registration process, and does not represent the actual velocity dispersion in the LMC.

In Figures 2 and 3 we present position vs. epoch diagrams for the QSO fields in R.A. ($\Delta\alpha\cos\delta$) and DEC ($\Delta\delta$), where $\Delta\alpha\cos\delta$ and $\Delta\delta$ represent the (X, Y) positions of the QSO on different CCD frames, relative to the barycenter of the SRF. These diagrams were obtained using individual position data for the QSO in each CCD image as a function of epoch. In Table 3 we give the mean barycentric positions of the QSOs per epoch, along with their mean errors (the errors of the averages). The heading N (sixth column) represents the sum of all data points (one per image) used to calculate the mean for each coordinate and corresponding epoch (first column). This sum is the same for both R.A. and DEC. Also shown (last column) are the CCD detectors used in each epoch. Symbol sizes in Figures 2 and 3 are proportional to the number of times the measurements yielded the same coordinate value for a particular epoch. The latter may be different for R.A. and DEC, since each point in Figures 2 and 3 represents a subset of data points in a small range of coordinates; thus, the number of points in the range may be different for R.A. and DEC, but the sum af all the points for a particular epoch is the same for both coordinates, as shown in Table 3. This is done to avoid point overlapping in the graph. The best-fit straight lines resulting from simple linear regression analysis on the data points are also shown. The negative values of the line slopes correspond to the PM of the barycenter of the LRS in each QSO field.

Table 4 summarizes our results for the (measured) PM of the LMC. Column 1 gives the quasar identification, Columns 2 and 3 the R.A. and DEC components (together with their standard deviations) of the LMC PM,

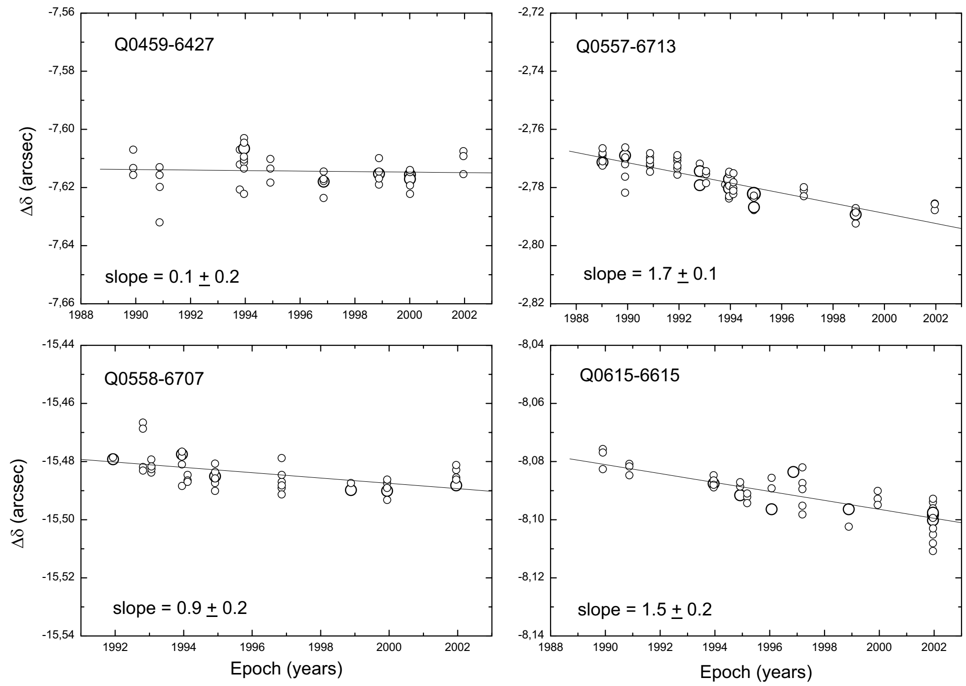

Fig. 3. Same as Figure 2 but for DEC ($\Delta\delta$).

TABLE 4

PROPER MOTION OF THE LMC (AS MEASURED)

Field ID	$\mu_\alpha \cos(\delta)$ mas yr^{-1}	μ_δ mas yr^{-1}	Frames	Epochs	Epoch Range
Q0459-6427	1.4 ± 0.2	0.1 ± 0.2	45	9	1989.91−2001.96
Q0557-6713	1.2 ± 0.2	1.7 ± 0.1	70	13	1989.02−2001.96
Q0558-6707	1.3 ± 0.2	0.9 ± 0.2	48	9	1992.81−2001.96
Q0615-6615	2.1 ± 0.2	1.5 ± 0.2	53	11	1989.90−2001.96

respectively, and, finally, Columns 4, 5, and 6 show the number of frames, the number of epochs, and the observation period, respectively. It should be noted that the rather small quoted errors for the PM come out directly from what the least-square fit yields as the uncertainty in the determination of the slope of the best fit line. The fact that the DEC component of the PM for Q0459-6427 in this table differs by more than 2σ from the rest, may be because this field is in a different location within the LMC relative to the rest of the fields, namely, to the NW of the LMC bar, whereas the other three fields are far to the NE of the LMC bar which means that it might be affected by local internal motions in the cloud of the type suggested by Piatek, Pryor, & Olszewski (2008). This topic probably deserves further studies on the dynamics of this LMC area (and others of similar type in it).

4. COMPARISON WITH PREVIOUS MEASUREMENTS

Table 5 lists the results of all the PM measurements that are known for the LMC with respect to either the center of the LMC or the corresponding field (indicated as "field"), with uncertainties of less than 1 mas yr^{-1} in both PM (μ) components, and the system of reference used in each case. The values for the LMC center are obtained by correcting the field PM for rotation of the LMC plane, and for perspective effects, as explained in

TABLE 5

HIGH PRECISION DETERMINATIONS OF THE PROPER MOTION FOR THE CENTER OF THE LMC

Source	LMC Adopted Parameters	$\mu_\alpha \cos(\delta)$ mas yr^{-1}	μ_δ mas yr^{-1}	Proper Motion System
Kroupa et al. (1994) (field)		$+1.3 \pm 0.6$	$+1.1 \pm 0.7$	PPM
Jones et al. (1994)	JKL94	$+1.37 \pm 0.28$	-0.18 ± 0.27	Galaxies
Kroupa & Bastian (1997) (field)		$+1.94 \pm 0.29$	-0.14 ± 0.36	Hipparcos
ALP00	JKL94	$+1.7 \pm 0.2$	$+2.9 \pm 0.2$	3 Quasars
PAM02	JKL94	$+2.0 \pm 0.2$	$+0.4 \pm 0.2$	1 Quasar
Drake et al. (2001)		$+1.4 \pm 0.4$	$+0.38 \pm 0.25$	Quasars
Kallivayalil et al. (2006)	vDM02	$+2.03 \pm 0.08$	$+0.44 \pm 0.05$	21 Quasars
PCM06 (weighted average)	JKL94	$+1.8 \pm 0.1$	$+0.9 \pm 0.05$	4 Quasars
Piatek et al. (2008)	vDM02	$+1.956 \pm 0.036$	$+0.435 \pm 0.036$	21 Quasars
CMP09	vDM02	$+1.82 \pm 0.13$	$+0.39 \pm 0.15$	1 Quasar
Vieira et al. (2010)	vDM02	$+1.89 \pm 0.27$	$+0.39 \pm 0.27$	SPM, Hipparcos
This work (weighted average)				
field		$+1.42 \pm 0.09$	$+1.32 \pm 0.09$	4 Quasars
	vDM02	$+1.46 \pm 0.09$	$+1.25 \pm 0.08$	4 Quasars
	JKL94	$+1.71 \pm 0.09$	$+0.92 \pm 0.07$	4 Quasars

the next section. The PM values shown in Table 5 for this work are those obtained using both the new input parameters for the LMC given by van der Marel et al. (2002, hereafter vDM02), and those given by Jones, Klemola, & Lin (1994, hereafter JKL94). This is done in order to facilitate comparison of our results with those by the rest of the authors. The adopted LMC parameters by these authors are:

LMC Center: (R.A., DEC) = $(81^\circ.90, -69^\circ.87) J2000.0$. Heliocentric distance of the LMC center: 50.1 kpc. Inclination of the disk: ($i = 34^\circ.7$). P.A. of the descending node: ($-50^\circ.1$), by vDM02.

LMC Center: (R.A., DEC) = $(80^\circ.25, -69^\circ.28) J1950.0$. Heliocentric distance of the LMC center: 50.1 kpc. Inclination of the disk: ($i = 27^\circ.0$). P.A. of the descending node: ($-10^\circ.0$), by JKL94.

Note that there is a significant difference between the values of the inclination of the disk and the P.A. of the descending node in both sets of parameters. This will notoriously affect the final results for the PM of the LMC center.

The total LMC PM values obtained here, for both vDM02 and JKL94 input parameters, amount to $\mu = (+1.92 \pm 0.08)$ mas yr^{-1}, with a position angle $\theta = 49^\circ.2 \pm 3^\circ.4$, and to $\mu = (+1.94 \pm 0.08)$ mas yr^{-1}, with a position angle $\theta = 61^\circ.5 \pm 3^\circ.2$, respectively. The position angle is measured eastward from the meridian joining the center of the LMC to the north pole.

The above total PM values are quite compatible with several theoretical models (Murai & Fujimoto 1980; Lin & Lynden Bell 1982; Shuter 1992; Gardiner, Sawa, & Fujimoto 1994), which predict a proper motion for the LMC in the range 1.5−2.0 mas yr^{-1}, but they are only marginally compatible with the $\theta \approx 90^\circ$ position angle predicted by the same models.

As seen from Table 5, the values of the PM determined by our group (for the JKL94 input LMC parameters) confirm the results of the PCM06 study and show a reasonable agreement with some of the available data. Our "field" results agree particularly well with those of Kroupa, Röser, & Bastian (1994), who used the *Positions and Proper Motions Star Catalog* (Röser & Bastian 1993, PPM) as reference system. On the other hand, there is a significant discrepancy with ALP00's result in DEC, and some discrepancy with the one-field results by CMP09 for QJ0557-6713.

The rest of the PM values in Table 5, that have been recently determined by other groups using QSOs, depart from our values by about 2σ (especially in DEC), with ours being the highest PM values and those by Piatek et al. (2008) the lowest and more recent values for the measured PM. The latter values are also in good agreement with other recent determination (except with ours in DEC). A possible explanation for this departure is that, in both previous sets of data, there may be systematic effects still present (despite some of

TABLE 6

PROPER MOTION AND SPACE VELOCITY RESULTS FOR THE LMC
VDM02 PARAMETERS AND $V_{\rm rot} = 50$ km s^{-1}

Parameter	Q0459-6427	Q0557-6713	Q0558-6707	Q0615-6615
$\Delta\mu_\alpha \cos\delta$, rotation correction (mas yr^{-1})	-0.17	0.17	0.17	0.17
$\Delta\mu_\delta$, rotation correction (mas yr^{-1})	-0.06	-0.14	-0.14	-0.15
$\mu_\alpha^{\rm Field} \cos\delta$, LMC centered (mas yr^{-1})	1.5 ± 0.2	1.0 ± 0.2	1.1 ± 0.2	1.9 ± 0.2
$\mu_\delta^{\rm Field}$, LMC centered (mas yr^{-1})	0.2 ± 0.2	1.9 ± 0.1	1.1 ± 0.2	1.7 ± 0.2
$\mu_\alpha^{\rm CM} \cos\delta$, LMC centered (mas yr^{-1})	1.4 ± 0.2	1.2 ± 0.1	1.2 ± 0.2	2.1 ± 0.2
$\mu_\delta^{\rm CM}$, LMC centered (mas yr^{-1})	0.4 ± 0.2	1.7 ± 0.1	0.9 ± 0.2	1.3 ± 0.1
$\mu_\alpha^{\rm GRF} \cos\delta$ (mas yr^{-1})	0.9 ± 0.1	0.7 ± 0.1	0.7 ± 0.1	1.6 ± 0.1
$\mu_\delta^{\rm GRF}$ (mas yr^{-1})	0.3 ± 0.2	1.6 ± 0.1	0.8 ± 0.2	1.1 ± 0.2
$\mu_l^{\rm GRF} \cos b$ (mas yr^{-1})	-0.4 ± 0.2	-1.7 ± 0.1	-0.9 ± 0.2	-1.4 ± 0.2
$\mu_b^{\rm GRF}$ (mas yr^{-1})	0.9 ± 0.1	0.5 ± 0.1	0.6 ± 0.1	1.4 ± 0.1
Π, velocity component (km s^{-1})	189 ± 28	199 ± 20	178 ± 25	306 ± 26
Θ, velocity component (km s^{-1})	65 ± 50	369 ± 28	182 ± 45	278 ± 36
Z, velocity component (km s^{-1})	133 ± 29	54 ± 21	80 ± 25	247 ± 27
$V_{\rm gc,r}$, radial velocity (km s^{-1})	86 ± 25	138 ± 18	106 ± 22	123 ± 24
$V_{\rm gc,t}$, transverse velocity (km s^{-1})	224 ± 32	399 ± 28	246 ± 38	466 ± 31

them having been corrected). In our set of data, a clear example of this kind of effect is the differential color refraction (DCR) whereas in Piatek et al. (2008) data it is the CCD charge transfer inefficiency. However, as mentioned before, both of these effects were corrected in the corresponding studies. In any case, to the best of our knowledge, the PM values in the present work are not greately affected by DCR, since the working set of images were all selected from those with hour angles less than 1 hr (in absolute value). The ground-based equipment (and its setup) used in our case, was a very stable one, with an optics with a minimal field distortion and whose parameters, as far as we know, were kept unchanged in all of our observing runs. The previously mentioned factors were quite appropriate for this type of astrometric studies.

5. SPATIAL VELOCITY OF THE LMC AND MASS OF THE GALAXY

Using the PM of the LMC determined in § 3, and the radial velocity of the center of the LMC (adopted from the literature), V_r, we can calculate the radial and tangential components of the LMC velocity, as seen from the center of the Galaxy. To do this we have followed the procedure outlined by JKL94. As mentioned before, in the calculations we used two sets of basic LMC parameters, namely, that adopted by vDM02, and that given by JKL94 (see previous section), along with radial velocities $V_r = 262.1$ km s^{-1} and $V_r = 250$ km s^{-1}, respectively. The rotational velocities of the LMC plane adopted for the range of distances from our studied fields to the LMC center (see § 4.1 in CMP09) were both $V_{\rm rot} = 50$ km s^{-1} and $V_{\rm rot} = 120$ km s^{-1}. The two sets of parameters were used to allow an easier comparison of our results with those of the rest of the authors in Table 5 and for following discussions.

In order to calculate the tangential and radial components of the LMC spatial velocity as seen from the Galactic center and with respect to the Galactic Rest Frame (GRF), from the previously measured PM, we have followed a series of steps, which were carried out through an ad-hoc computer software written by the author (MHP). These include: a correction of the PM values for the rotation of the LMC plane; a transformation of the corrected PM into R.A. and DEC velocities centered on the field; a transformation of these two velocity components, into heliocentric (hc) galactic longitudinal and latitudinal velocity components for the center of the LMC; a transformation of the previous velocity components into their galactocentric (gc) counterparts which, in turn, were combined to derive the transverse velocity, ($V_{\rm gc,t}$) of the LMC center with respect to the Galactic center. Similarly, in order to obtain the galactocentric radial velocity ($V_{\rm gc,r}$) for the LMC center, we

TABLE 7

PROPER MOTION AND SPACE VELOCITY RESULTS FOR THE LMC
JLK94 PARAMETERS AND $V_{\rm rot} = 50$ km s^{-1}

Parameter	Q0459-6427	Q0557-6713	Q0558-6707	Q0615-6615
$\Delta\mu_\alpha \cos\delta$, rotation correction (mas yr^{-1})	-0.17	-0.11	-0.11	-0.12
$\Delta\mu_\delta$, rotation correction (mas yr^{-1})	-0.09	0.18	0.18	0.18
$\mu_\alpha^{\rm Field} \cos\delta$, LMC centered (mas yr^{-1})	1.5 ± 0.2	1.3 ± 0.2	1.4 ± 0.2	2.2 ± 0.2
$\mu_\delta^{\rm Field}$, LMC centered (mas yr^{-1})	0.2 ± 0.2	1.6 ± 0.1	0.7 ± 0.2	1.4 ± 0.2
$\mu_\alpha^{\rm CM} \cos\delta$, LMC centered (mas yr^{-1})	1.5 ± 0.2	1.5 ± 0.1	1.5 ± 0.2	2.4 ± 0.2
$\mu_\delta^{\rm CM}$, LMC centered (mas yr^{-1})	0.4 ± 0.2	1.3 ± 0.1	0.5 ± 0.2	0.9 ± 0.1
$\mu_\alpha^{\rm GRF} \cos\delta$ (mas yr^{-1})	1.0 ± 0.1	1.0 ± 0.1	1.0 ± 0.1	1.9 ± 0.1
$\mu_\delta^{\rm GRF}$ (mas yr^{-1})	0.3 ± 0.2	1.2 ± 0.1	0.4 ± 0.2	0.7 ± 0.2
$\mu_l^{\rm GRF} \cos b$ (mas yr^{-1})	-0.4 ± 0.2	-1.4 ± 0.1	-0.6 ± 0.2	-1.1 ± 0.2
$\mu_b^{\rm GRF}$ (mas yr^{-1})	0.9 ± 0.1	0.8 ± 0.1	0.9 ± 0.1	1.7 ± 0.1
Π, velocity component (km s^{-1})	189 ± 30	218 ± 21	195 ± 26	325 ± 27
Θ, velocity component (km s^{-1})	70 ± 53	291 ± 29	105 ± 46	193 ± 37
Z, velocity component (km s^{-1})	148 ± 30	124 ± 22	147 ± 26	313 ± 28
$V_{\rm gc,r}$, radial velocity (km s^{-1})	76 ± 27	114 ± 20	81 ± 24	97 ± 25
$V_{\rm gc,t}$, transverse velocity (km s^{-1})	239 ± 33	367 ± 27	253 ± 31	481 ± 30

applied the previous procedure to the radial velocity of each field (V_r), whose values were adopted in such a way as to reproduce the nominal radial velocity of the LMC center adopted from the literature. The transverse and radial components are finally combined to obtain the spatial velocity vector of the LMC center. The reader is referred to ALP00, PAM02 and PCM06 for more details of the procedure. The results from these calculations are listed in Tables 6 and 7. These two tables also show the equatorial and galactic coordinate components of the PM relative to the GRF (representing the motion of the cloud as seen from a reference point that is stationary with respect to the Galactic center and which is located at the instantaneous solar position), and the Π, Θ and Z galactocentric space velocity components of the LMC in a rectangular Cartesian coordinate system centered on the LMC (as defined by Schweitzer et al. (1995) for the Sculptor dwarf spheroidal galaxy and described by PCM06 for the LMC).

If we assume that the LMC is gravitationally bound to, and in an elliptical orbit, around the Galaxy, and that the mass of the Galaxy is contained within 50 kpc of the galactic center, we can calculate its lower mass limit through the following expression for a point-mass galactic potential:

$$M_{\rm G} = (r_{\rm LMC}/2G)[V_{\rm gc,r} + V_{\rm gc,\,t}(1 - r^2_{\rm LMC}/r^2_a)]/(1 - r_{\rm LMC}/r_a)\,,$$

where r_a is the LMC apogalacticon distance and $r_{\rm LMC}$ its present distance.

For $r_a = 300$ kpc (Galaxy's tidal radius), the two sets of LMC input parameters quoted above, respectively, and rotation velocities of 50 and 120 km s^{-1}, we obtain the results shown in Tables 8 and 9,

Values in Table 8 (for the vDM02 LMC input parameters) result in weighted averages of: $\langle M_{\rm G}\rangle = (6.6 \pm 0.7) \times 10^{11}\ M_\odot$ and $\langle M_{\rm G}\rangle = (8.8 \pm 0.8) \times 10^{11}\ M_\odot$, for the mass of our Galaxy enclosed within 50 kpc, for the two mentioned rotation velocities, respectively. Likewise, values shown in Table 9 (for the JKL94 LMC input parameters) resulted in weighted averages of: $\langle M_{\rm G}\rangle = (6.4 \pm 0.6) \times 10^{11}\ M_\odot$ and $\langle M_{\rm G}\rangle = (7.1 \pm 0.6) \times 10^{11}\ M_\odot$, respectively.

One of the reasons why there are a couple of velocities (mainly tangential velocities) and masses of the Galaxy, derived from our four QSO fields, whose differences are greater than 2σ in Tables 8 and 9, may be due to local internal motions in that area of the LMC, as those suggested by Piatek et al. (2008), especially considering that our four fields are located at the northern side of the LMC bar, albeit at twice the distance from the center of mass of the LMC as those used by the latter authors. This is the area on the LMC,

TABLE 8

MASS OF THE GALAXY FOR TWO LMC ROTATIONAL VELOCITIES (VDM02 PARAMETERS)

Parameter	Q0459-6427	Q0557-6713	Q0558-6707	Q0615-6615
For $V_{\rm rot} = 50$ km s^{-1}				
$V_{\rm gc,r}$, LMC galactocentric velocity (km s^{-1})	86 ± 25	138 ± 18	106 ± 22	123 ± 24
$V_{\rm gc,t}$, LMC galactocentric velocity (km s^{-1})	224 ± 32	399 ± 28	246 ± 38	466 ± 31
$M_{\rm G}$, mass of the Galaxy in $10^{11}\times\ M_\odot$	(3.9 ± 1.0)	(12 ± 2)	(4.9 ± 1.3)	(16 ± 2)
For $V_{\rm rot} = 120$ km s^{-1}				
$V_{\rm gc,r}$, LMC galactocentric velocity (km s^{-1})	91 ± 25	146 ± 18	114 ± 22	132 ± 24
$V_{\rm gc,t}$, LMC galactocentric velocity (km s^{-1})	283 ± 32	428 ± 28	256 ± 43	466 ± 33
$M_{\rm G}$, mass of the Galaxy in $10^{11}\times\ M_\odot$	(6.0 ± 1.3)	(14 ± 2)	(5.4 ± 1.5)	(16 ± 2)

TABLE 9

MASS OF THE GALAXY FOR TWO LMC ROTATIONAL VELOCITIES (JKL94 PARAMETERS)

Parameter	Q0459-6427	Q0557-6713	Q0558-6707	Q0615-6615
For $V_{\rm rot} = 50$ km s^{-1}				
$V_{\rm gc,r}$, LMC galactocentric velocity (km s^{-1})	76 ± 27	114 ± 20	81 ± 24	97 ± 25
$V_{\rm gc,t}$, LMC galactocentric velocity (km s^{-1})	239 ± 33	367 ± 27	253 ± 31	481 ± 30
$M_{\rm G}$, mass of the Galaxy in $10^{11}\times\ M_\odot$	(3.9 ± 1.1)	(9.2 ± 1.4)	(4.4 ± 1.1)	(16 ± 2)
For $V_{\rm rot} = 120$ km s^{-1}				
$V_{\rm gc,r}$, LMC galactocentric velocity (km s^{-1})	82 ± 27	103 ± 20	71 ± 24	87 ± 25
$V_{\rm gc,t}$, LMC galactocentric velocity (km s^{-1})	299 ± 34	343 ± 26	265 ± 27	488 ± 29
$M_{\rm G}$, mass of the Galaxy in $10^{11}\times\ M_\odot$	(6.1 ± 1.4)	(8.0 ± 1.2)	(4.8 ± 1.0)	(16 ± 2)

showing greater internal motions (Piatek et al. 2008). We remind the reader that in order to determine the mentioned velocities, we had to correct for perspective effects and assume a constant rotation velocity of the LMC plane for all the QSO fields, which would introduce an error in the center of mass PM and consequently in the derived tangential velocities, should local internal motions departing from the assumed constant rotation velocity be present. Another possible error factor (among several others) affecting the derived velocities and masses, especially in extreme cases as that for the field Q0615-6615, could be optical brightness variability, of the fiducial QSO, with time (observing epoch), which is known to occur in some QSOs (i.e. Geha et al. 2003), that could affect the QSO centering process, contaminating the PM results for that particular field. This variability hypothesis should be tested for this particular QSO.

Although slightly larger (specially those for $V_{\rm rot} = 120$ km s^{-1}), the quoted results are compatible with the theoretical $5.5 \times 10^{11}\ M_\odot$ value for the upper mass limit of the Galaxy (Sakamoto, Chiba, & Beers 2003), and with the assumption that the LMC is bound to the Galaxy.

6. CONCLUSIONS

1. Our results, obtained from re-processing the data directly from the original images in order to measure the PM of each LMC field relative to the QSO for different epochs, confirm the results by PCM06 obtained from the (X, Y) coordinates previously processed by the original authors in ALP00. This supports the idea mentioned in § 6.1 by PCM06, where they state that the "ALP00-PAM02 discrepancy" did not originate

in the data itself but rather in the data processing by ALP00. This is because in the present work we read the images anew and re-process them from scratch, obtaining basically the same results as those by PCM06.

2. Besides, the procedure to register the individual images into the Standard Frame of Reference, used in this work, through a third degree polynomial, yields basically the same results (although with lower errors) as those by PCM006, meaning that the above discrepancy does not arise from the registration process.

3. Our results here are in a better agreement with those by other authors, in particular with the result given by Kroupa et al. (1994), as well as with several theoretical models, when using the JKL94 LMC input parameters rather than the more recent ones by vDM02.

4. There might be systematic errors still present in some of the PM values using the "quasar method", in Table 5, which would account for some observed marginal differences (of the order of 2σ) in PM, especially in DEC.

5. In reference to the stream of galaxies orbiting around our Galaxy, which would include the LMC, SMC, Draco and Ursa Minor, and possibly Carina and Sculptor galaxies, proposed by Lynden-Bell & Lynden-Bell (1995), and according to the results in the present work, we can conclude that the LMC does not seem to be a member of the proposed stream, because our measured values for μ and θ are at least (considering both sets of LMC input parameters) 5.2σ and 8.9σ away from the predicted values of $\mu = +1.5$ mas yr^{-1} and $\theta = 90°$.

6. The marginal discrepancy of our results from those by CMP09 (especially in DEC) for the same QSO field, has so far no explanation. It might be interesting to note though, that between the present study and that by CMP09 there are important observing setup differences, among them, a different telescope, telescope setup and detector equipment as well as a different set of LRS stars, for the QJ0557-6713 field and, in the present work, a longer observing time baseline and a greater number of observing epochs, for the above field. It is also interesting to note that, despite the short baseline and the fact that only one LMC field was included in this study, the PM values determined by CMP09 are closer to recently measured values for the LMC center of mass than ours.

7. Summing up, our PM and space velocity values support the idea that the LMC is indeed gravitationally bound to our Galaxy.

M.H.P. is greatful of the support by the Universidad de Tarapacá research fund (project # 4721-09). The author wishes to thank to an anonymous referee for helpful suggestions which improved this paper. It is also a pleasure to thank T. Martínez for helping with data processing.

REFERENCES

Anguita, C., Loyola, P., & Pedreros, M. H. 2000, AJ, 120, 845 (ALP00)
Costa, E., et al. 2009, AJ, 137, 4339 (CMP09)
Drake, A. J., Cook, K. H., Alcock, C., Axelrod, T. S., Geha, M., & MACHO Collaboration 2001, Bull. Am. Astron. Soc., 33, 1379
Gardiner, L. T., Sawa, T., & Fujimoto, M. 1994, MNRAS, 266, 567
Geha, M., et al. 2003, AJ, 125, 1
Jones, B. F., Klemola, A. R., & Lin, D. N. C. 1994, AJ, 107, 1333 (JKL94)
Kallivayalil, N., van der Marel, R. P., Alcock, C., Axelrod, T., Cook, K. H., Drake, A. J., & Geha, M. 2006, ApJ, 638, 772
Kroupa, P., & Bastian, U. 1997, New Astron., 2, 77
Kroupa, P., Röser, S., & Bastian, U. 1994, MNRAS, 266, 412
Lin, D. N. C., & Lynden-Bell, D. 1982, MNRAS, 198, 707
Lynden-Bell, D., & Lynden-Bell, R. M. 1995, MNRAS, 275, 429
Murai, T., & Fujimoto, M. 1980, PASJ, 32, 581
Pedreros, M. H., Anguita, C., & Maza, J. 2002, AJ, 123, 1971 (PAM02)
Pedreros, M. H., Costa, E., & Méndez, R. A. 2006, AJ, 131, 1461 (PCM06)
Piatek, S., Pryor, C., & Olszewski, E. W. 2008, AJ, 135, 1024
Röser, S., & Bastian, U. 1993, Bull. Inf. CDS, 42, 11 (PPM)

Sakamoto, T., Chiba, M., & Beers, T. C. 2003, A&A, 397, 889
Schweitzer, A. E., Cudworth, K. M., Majewski, S. R., & Suntzeff, N. B. 1995, AJ, 110, 2747
Shuter, W. L. H. 1992, ApJ, 386, 101
Stetson, P. B. 1987, PASP, 99, 191
van der Marel, R. P., Alves, D. R., Hardy, E., & Suntzeff, N. B. 2002, AJ, 124, 2639 (vDM02)
Vieira, K., et al. 2010, AJ, 140, 1934

Mario H. Pedreros: Departamento de Física, Facultad de Ciencias, Universidad de Tarapacá, Casilla 7-D, Arica, Chile (mpedrero@uta.cl).